When Does Catalysis with Transition Metal Complexes Turn into Catalysis by Nanoparticles?

Vries, Johannes G. de

Published in:
Selective Nanocatalysts and Nanoscience: Concepts for Heterogeneous and Homogeneous Catalysis

Publication date:
2011

3
When Does Catalysis with Transition Metal Complexes Turn into Catalysis by Nanoparticles?

Johannes G. de Vries

3.1
Introduction

Catalysis is essential in the production of chemicals, particularly in the production of bulk chemicals, but increasingly also for the production of fine chemicals [1]. If we confine ourselves to metal-based catalysts, we distinguish three forms of catalysis: heterogeneous catalysis, homogeneous catalysis, and catalysis with nanoparticles. The latter class may be further subdivided in catalysis with soluble metal nanoparticles and catalysis with supported metal nanoparticles, although the latter is usually seen as heterogeneous catalysis.

3.1.1
Homogeneous Catalysis

The catalyst used in homogeneous catalysis is typically a transition metal complex in which the central metal atom is ligated by one or more organic ligands that bind via one or more coordinating atoms to the metal [2]. The metal can be in the zero oxidation state or it can be in a higher oxidation state, in which case it has counterions. The counterions may bind to the metal like a ligand; this occurs with halides and carboxylates. The counterion may also have a highly delocalized charge such as in BF_4^- or PF_6^-; in that case, the counterion does not bind directly to the metal atom. This results in the formation of cationic complexes.

The advantages of homogeneous catalysis are the following:

1) The catalyst is in the same phase as the substrate, which leads to a very efficient catalysis that is not hindered by diffusion problems.

2) Every single metal atom is catalytically active and has the same catalytic performance.

3) Rate and selectivity of the catalyst can be altered by changing the metal, the counterion, and the ligand. Since there is a huge diversity of ligands accessible by organic synthesis, this property makes it almost always possible to develop

Selective Nanocatalysts and Nanoscience, First Edition. Edited by Adriano Zecchina, Silvia Bordiga, Elena Groppo.

an economic process by screening these variables. This process can be accelerated by the use of high-throughput experimentation.

4) Research into the mechanism is relatively easy because of the molecular nature of the catalyst, which allows the use of spectroscopic techniques such as NMR.

The most important disadvantage of homogeneous catalysis is the instability of the catalyst. All three classes of catalysts can be inhibited by reaction with, or adsorption on the surface of catalyst poisons. However, a deactivation mechanism that is unique for homogeneous catalysis is through the loss of ligands. This may happen simply by dissociation or by reaction of an external reagent with the ligand. Once the metal complex becomes unsaturated, it can start to dimerize by a number of different mechanisms. This agglomerization can continue to form multimetallic clusters. If the metal is in the zero oxidation state, this process can lead to the formation of nanoparticles and eventually to the formation of metal crystals that precipitate, leading to an effective halt of the catalysis.

Although many articles, particularly those describing the immobilization of homogeneous catalysts, claim that separating the homogeneous catalyst from the product is a major problem, this is in fact not true. In bulk chemical processes, the catalyst and the product are usually separated by distillation. This can become a problem if the molecular weight of the product is too high leading to high temperatures during the distillation process, which may lead to catalyst decomposition. However, the molecular weight of most bulk chemical products is quite low. In fact there are 21 different bulk chemical processes based on homogeneous catalysis, testifying to the fact that catalyst separation and recycle is not a major problem. In fine chemicals, the product is isolated either by distillation or crystallization. Since the catalyst is usually not recycled, there is no real problem.

3.1.2 Heterogeneous Metal Catalysis

A heterogeneous metal catalyst usually consists of crystals of a metal or agglomerates of more than one metal that are deposited on a solid carrier material which usually is a silica or aluminum oxide or active carbon, although other supports are also known [3].

The advantages of heterogeneous catalysis are the following:

1) The catalysts are highly robust, which allows their use at high temperatures, which may lead to very high rates.
2) The catalysts are not easily deactivated, which allows their use for prolonged periods of time.

The main disadvantage of heterogeneous catalysts is the limited number of parameters available for attenuating their activity and selectivity. Addition of other metals, variation in the size of the crystallites, and change in the carrier material are the only available variables. Another disadvantage is the fact that only the metal

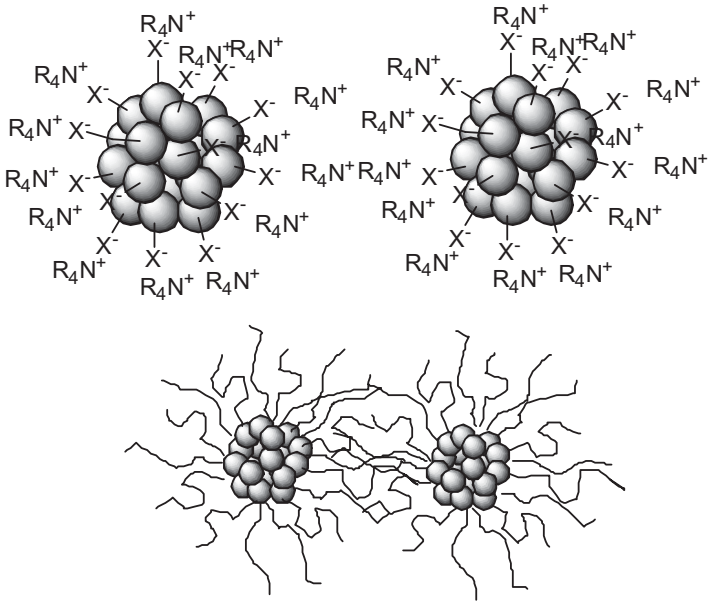

Figure 3.1 Stabilization of metal nanoparticles by tetra-alkylammonium halides or long-chain surfactants or amines.

atoms on the outside can possibly be active. Very often it is only the metal atoms at defects such as kinks and steps that are active.

3.1.3
Catalysis with Soluble Metal Nanoparticles

Nanoparticles are agglomerates of metals, usually in the zero oxidation state. They are prevented from growing to larger crystals by the presence of stabilizing ligands that form a steric or a charge barrier between them (Figure 3.1). Common stabilizers are tetra-alkylammonium halides or carboxylates, anionic surfactants, nitrogen, or phosphorus ligands carrying long alkyl chain or aryl rings or polar polymers, such as PVP. Their size is usually somewhere between 1 and 100 nm. Metal oxides and metal salts can also form nanoparticles. Nanoparticles can be prepared on purpose, for instance by reduction of a metal salt in the presence of a stabilizer. They can also be formed accidentally during catalysis.

The advantages of their use as catalysts can be described as follows:

1) The catalysts are soluble in the same reaction medium as the substrate; thus there are no diffusion limitations.
2) The stabilizing ligands tend to be bulk chemicals and are thus orders of magnitude cheaper than commonly used ligands in homogeneous catalysis.
3) The stabilizing ligands are usually not strongly bound and hence are easily displaced by the substrate.

4) Small-sized nanoparticles tend to be faster catalysts than the metal complex catalyst in the same reaction.

Metal nanoparticles have been used as catalyst in many types of reactions [4]. The disadvantages of the use of nanoparticle catalysts are their instability; particularly at higher temperatures, they tend to grow to larger size in a process known as Oswald ripening, which will end in their precipitation. On the other hand, if precipitation can be prevented *during* the reaction it can actually be used to good advantage to isolate the catalyst *after* the reaction.

Metal nanoparticles can be seen as the bridge between homogeneous and heterogeneous catalysis. They are soluble in the same medium as the substrate, they can react as a homogeneous catalyst for instance in the Heck reaction, but they also have a surface and thus can react as a heterogeneous catalyst as in hydrogenation reactions.

3.1.4 The Border between the Three Forms of Catalysis

Many cases are known where a catalyst in the form of a transition metal complex was converted into nanoparticles during a catalytic reaction. Often researchers are blissfully unaware of this fact. Several cases will be described in this chapter. Heterogeneous catalysts can also be solubilized. This is commonly referred to as leaching. Lesser known is that in many cases, it is in fact the leached metal that is responsible for the catalysis. This is true for most oxidation processes [5], but also for palladium-catalyzed C–C bond formation reactions. It is also possible that all or part of the metal from the heterogeneous catalyst is solubilized in the form of nanoparticles.

It is often not easy to distinguish between the three forms of catalysis. Finke devised a number of tests that can aid in making the distinction between catalysis by complexes and catalysis on surfaces [6]. He also stresses the fact that the distinction can never be made on the basis of a single test as each test has its own flaws.

1) *Visible evidence*: TEM will show the presence of nanoparticles. Light diffraction can also be used for this purpose.

2) *Kinetic evidence*: If nanoparticles are the active catalyst and are formed during the reaction an induction period may be apparent, often leading to a sigmoidal curve. The kinetics is sometimes irreproducible.

3) Quantitative poisoning studies (CS_2, or other sulfur-containing compounds, PPh_3,); Hg poisoning.

4) The identity of the true catalyst must be consistent with all the data.

This chapter will describe several cases where the catalysis operates at the borderline between homogeneous catalysis and catalysis by nanoparticles and also some cases where heterogeneous catalysts turn into nanoparticles catalysts.

3.2
Nanoparticles vs. Homogeneous Catalysts in C–C Bond-Forming Reactions

Most metal-catalyzed C–C bond-forming reactions catalyzed by transition metal catalysts proceed through a catalytic cycle in which the catalyst changes oxidation state, usually alternating between the zero and the plus two oxidation states. This is a typical situation in which catalyst destablization may occur. Whereas the +2 oxidation state usually results in quite stable complexes in view of the electron-donating nature of all ligands, the metal–ligand bond strength in the zero oxidation state may considerably be reduced leading to ligand dissociation and opening the way to clustering and possibly precipitation of metal crystals. This phenomenon is particularly prevalent with palladium.

3.2.1
The Heck–Mizoroki Reaction

In the Heck–Mizoroki reaction, a bond is formed between an olefin and an aromatic compound, which contains a leaving group [7]. In Heck's original version, these were mainly iodide and bromide [8]. Later versions were developed in which the leaving group could also be chloride, triflate, diazonium salts, iodonium salts, tosylate, acid chloride, anhydride, alkenyl esters, sulfonylchloride, or silanols [7] (Scheme 3.1).

Reetz and Beller independently have shown that the Heck reaction can also be catalyzed by preformed palladium nanoparticles that are stabilized by tetra-alkylammonium halides or by polar polymers such as PVP [9, 10]. The rate of these reactions was not higher than those catalyzed by palladium phosphine complexes and thus these results initially did not attract much attention.

The first sign that palladium nanoparticles were more prevalent in the Heck reaction came from the research of Reetz and coworkers on the Heck reaction using Jeffery conditions [11]. In this variant, no ligand is used – just palladium acetate, an inorganic potassium base, and a tetra-alkylammonium salt which was originally intended to aid the solubilization of the inorganic base in the reaction

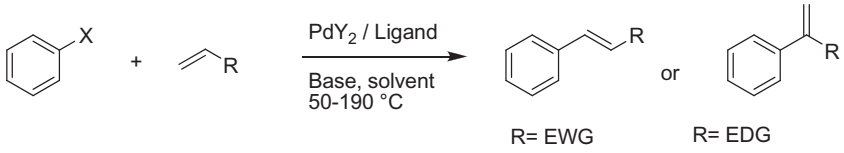

X= I, Br, Cl, $N_2^+X^-$, OSO_2R, COCl, $CO_2C(O)Ar$, $CO_2CH{=}CHR$,
R= H, alkyl, aryl, electron withdrawing group (EWG) or electron donating group (EDG)
Y= Cl, OAc, dba
Ligand = none, phosphine, phosphite, phosphoramidite
Base= Et_3N, $NaHCO_3$, K_2CO_3, KOAc, K_3PO_4

Scheme 3.1 The Heck–Mizoroki reaction.

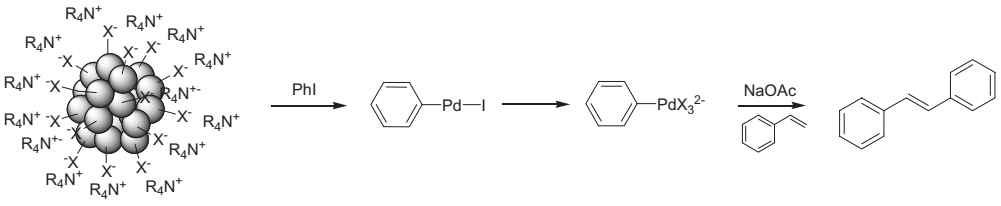

Scheme 3.2 Palladium nanoparticles as stoichiometric catalysts for the Heck reaction.

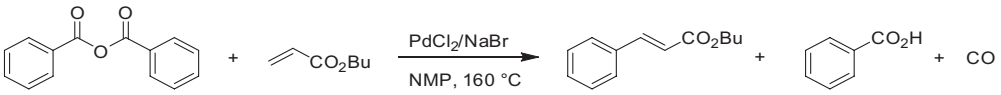

Scheme 3.3 Heck reaction on aromatic anhydrides.

medium [12]. Using TEM, Reetz showed the presence of palladium nanoparticles in these reactions [11]. He went one step further and reacted preformed palladium nanoparticles with an equivalent of iodobenzene (Scheme 3.2). Following this reaction with UV and ^{13}C NMR, he showed that the typical UV spectrum of the nanoparticles disappeared and that in the NMR the peaks of iodobenzene disappeared and at the same time a new set of peaks appeared which he attributed to an aryl palladium species, most likely $(PhPdI_3)^{2-}$. Adding styrene and NaOAc to this solution led to formation of the Heck product stilbene.

De Vries and coworkers have pioneered the use of aromatic anhydrides as arylating agents in the Heck reaction in an attempt to reduce the stoichiometric amount of salt waste that accompanies the formation of the Heck product [13]. In this reaction, CO and benzoic acid are the side products. The CO can be burned to CO_2 and the benzoic acid can be recycled back to the anhydride. This is one of the few Heck reactions that operate without base (Scheme 3.3).

One of the many other surprising elements regarding this reaction is the fact that it does not proceed in the presence of ligands, such as PPh_3. Later it was found that the presence of ligands prevents the decarbonylation reaction, which is a necessary step in the catalytic cycle [14]. However, the reaction is cocatalyzed by small amounts of chloride or better bromide salts. The maximum effect was obtained at a halide/palladium ratio of 4, which suggests an action at the level of the catalyst. Intrigued by these findings, the reaction was examined spectroscopically using TEM, EDX, EXAFS, and electrospray MS. TEM clearly showed the presence of nanoparticles, which was also confirmed by the EXAFS results that showed a Pd–Pd number of 8–12. In addition, the EXAFS showed the presence of multiple Pd–halide bonds and a single palladium–carbon bond. Most revealing was the electrospray MS, which showed the presence of a number of anionic monomeric and dimeric palladium species. One of these was $PhPdCl_2^-$ (in this reaction NaCl was used as additive). It is quite possible that this compound is present in solution as a dimeric species. These findings suggest that although a

very large amount of the palladium is actually in the form of soluble nanoparticles, the actual catalysis proceeds via monomeric, or possibly dimeric, anionic species [15]. The role of the halide salt may be twofold: it stabilizes the colloids, thus preventing their further growth to palladium black, and they function as ligand for palladium in the actual catalytic cycle, which proceeds through anionic intermediates, in analogy with the proposals of Amatore and Jutand for the catalysis by palladium–phosphine complexes [16]. These findings led them to examine the Heck reaction under Jeffery conditions using TEM and ES-MS. They could confirm the presence of nanoparticles in the TEM. In the ES-MS, they detected the presence of $PhPdI_2^-$. In addition to that, a large peak attributable to PdI_3^- is visible [17]. Independent work performed by Evans using EXAFS showed the presence of large amounts of the dimeric species $Pd_2I_6^-$ in this reaction [18].

The above findings led them propose the following mechanism for these ligand-free Heck reactions (Scheme 3.4) [15, 17].

In the first phase of the reaction, Pd(II) is reduced to Pd(0) [19]. During the first 5 min of the reaction, they observed $([H_2O]PdOAc)^-$, which is a rare example of an anionic palladium(0) complex. This complex may undergo oxidative addition of aryl iodide to form $ArPdI_2^-$. This species and all other underligated species may well have a molecule of solvent (NMP, DMF) coordinated or they may be present as dimers [18]. The rest of the catalytic cycle proceeds along conventional lines via

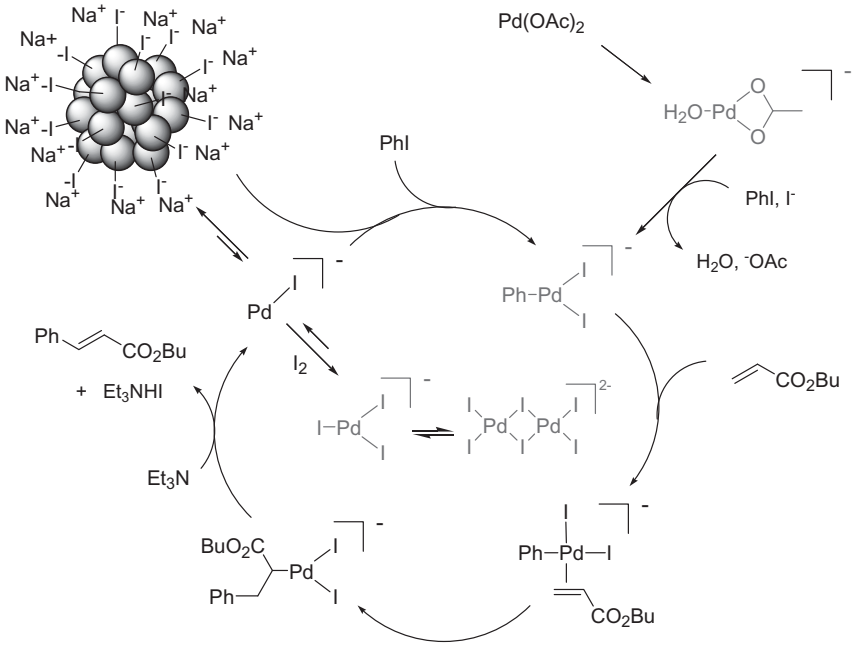

Scheme 3.4 Mechanism for the ligand-free Heck reaction. Intermediates in gray were observed by ES-MS.

olefin complex formation, olefin insertion, and beta-hydride elimination. However, all these intermediates are anionic. Hartwig recently showed that olefin insertion is much faster with these anionic complexes than with conventional phosphine-ligated neutral palladium complexes [20]. After beta-hydride elimination, the anionic palladium species left is highly underligated. At this stage, three pathways are possible: (i) reaction with I_2 to form PdI_3^- or more likely its dimer as found by Evans; (ii) formation of soluble nanoparticles; (iii) reaction with ArI. Since oxidative addition is fast with ArI, we would expect that in this case during the early stages of the reaction hardly any palladium colloids will be formed, depending on the substrate-to-catalyst (S/C) ratio. This is in agreement with the findings from Evans. At this point, it is unclear where the I_2 comes from; traces of oxygen may seem the most likely explanation [21]. However, Schmidt has proposed that it may arise from the formation of biphenyl [22]. This is a net reduction, which leads to the formation of Pd(II). Indeed, Schmidt has shown that the Heck reaction with ligand-less palladium actually is accelerated by the addition of sodium formate, which quickly reduces the formed Pd(II) back to Pd(0). At the end of the reaction, the nanoparticles will form rapidly, leading eventually to the formation of palladium black. Once the nanoparticles form, they can be solubilized again by reaction with aryl iodide under formation of $ArPdI_2^-$. The presence of the anion is essential to aid in the process of the solubilization.

Till recently, use of Jeffery conditions for the Heck reaction on aryl bromides was impossible. Here the oxidative addition of the aryl bromide is rate determining. The consequence is that all palladium will be present in the zero oxidation state and hence rapidly forms nanoparticles. The oxidative addition of the aryl halide will take out the palladium atoms at the rim of the nanoparticles in the form of $ArPdBr_2^-$. As this solubilization by oxidative addition is not fast enough, the Oswald ripening becomes the prevailing process, eventually leading to precipitation of palladium black. Scheme 3.5 shows this problem in a simplified form.

The DSM group tried a number of common stabilizers in order to prevent the further growth of the nanoparticles, but this was not terribly effective. In addition,

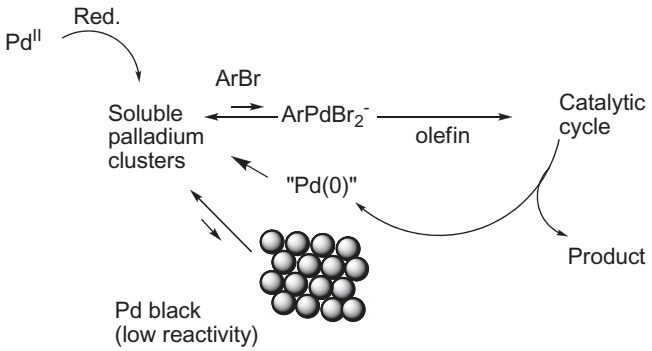

Scheme 3.5 Competition between oxidative addition of ArBr and Oswald ripening determines the size of the nanoparticles.

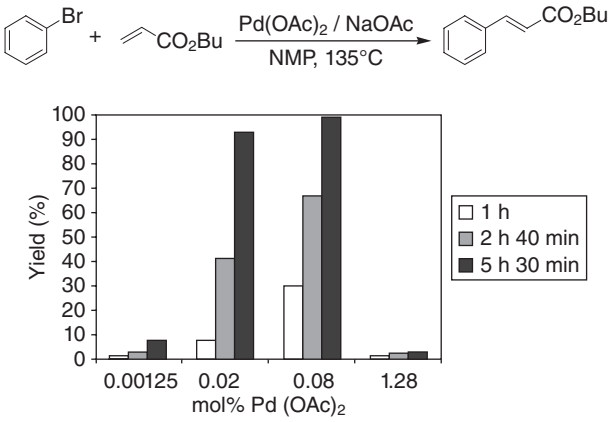

Figure 3.2 Effect of mol% of palladium on the rate of the ligand-free Heck reaction.

these additives defeat the purpose of the ligand-free Heck reaction, which is so convenient for synthetic purposes and even large-scale production in view of its easy workup. Looking again at Scheme 3.5, another solution to this problem presents itself. Whereas the Heck reaction is first order or possibly half order in palladium, the formation of the nanoparticles must follow a higher order. This suggests that lowering the palladium concentration might actually help in balancing the size reduction of the nanoparticles against their natural tendency to grow. Thus, four different palladium concentrations were tested in the ligand-free Heck reaction between bromobenzene and butyl acrylate. The rate of the reaction at these four concentrations is graphically depicted in Figure 3.2 [23].

At 1.28 mol%, the reaction is very slow, and the reason for this is clearly visible: almost immediately after the start of the reaction, palladium black started to form. However, at lower concentrations between 0.01 and 0.1 mol% of palladium, the reaction ran very smoothly without any precipitation of palladium during the reaction. These very low loadings were described by the authors and earlier by Beletskaya as "homeopathic palladium." Much lower amounts of catalyst are possible but need higher temperatures for a decent rate [24]. Comparing the rate at 0.08 and 0.02 mol%, it is clear that the turnover frequency (TOF) of the reaction actually increases by lowering the amount of palladium. This can be simply explained by the fact that the lower the palladium concentration the smaller the nanoparticles will be as their rate of formation is retarded. The smaller the nanoparticles, the more surface atoms will be available for catalysis and the higher the TOF. This phenomenon of increasing TOF with decreasing catalyst/substrate ratio is a telltale sign for the involvement of nanoparticles in these reactions. In fact, looking back at the many hundreds of publications describing new types of catalysts in the Heck reaction, this phenomenon is encountered quite frequently, suggesting that all high-temperature Heck reactions function via this mechanism [25]. We will discus some selected examples below.

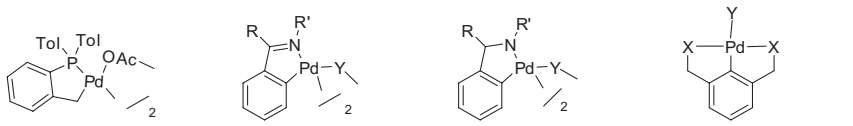

Herrmann-Beller palladacycle

R = alkyl, aryl; R' = alkyl aryl, Oalkyl; Y = Cl, Br, I, OTf, OAc; X = NR_2, PR_2, $OP(OR)_2$, SR

Figure 3.3 Palladacycles and pincer complexes used as catalysts in the Heck reaction.

The homeopathic palladium approach initially was not very successful for the conversion of aryl chlorides. The problem may be that here the oxidative addition step is even slower than that with the aryl bromides. Koehler found that very low amounts of $Pd(OAc)_2$ can indeed be used as catalyst for Heck reactions on aryl chloride if the reactions are carried out at higher temperatures (160 °C) [26]. In addition, he used tetra-alkylammonium bromide as stabilizer and finally he performs these reactions in air. The function of air is not entirely clear. It may actually oxidize the palladium on the outer rim of the nanoparticles and thus contribute to keep down the size of the nanoparticles. An alternative explanation would be the formation of palladium–oxygen complexes.

When Herrmann and Beller introduced the use of palladacycles as catalyst for the Heck reaction, this caused quite a bit of excitement and actually blew new life in an area that had been dormant for long [27]. Many research groups started to work in this area, and quite a few palladacyles and pincer complexes were reported that showed excellent activity in the Heck reaction (Figure 3.3) [28].

Immediately after their publication, a long debate ensued about the possible mechanism of the Heck reaction catalyzed by these complexes. Initial proposals by Herrmann and Beller, but also by Shaw, involved a Pd(II)/Pd(IV) cycle [27, 29]. It was shown by Hartwig that palladacycles are actually quite easily reduced to Pd(0) [30], which led to speculation about other possible mechanisms [31]. Interestingly an increase in TOF with increasing S/C ratio was already observed upon use of this catalyst in the Heck reaction. The story took an interesting twist when Nowotny and coworkers investigated the Heck reaction between iodobenzene and styrene using an immobilized palladacycle (Scheme 3.6) [32]. The obvious purpose of the study was to examine the recyclability of the immobilized catalyst. Disappointingly, the authors found that the solid catalyst lost all of its activity after the second run. However, the filtrate retained all the activity of the original catalyst. In addition, the second reaction catalyzed by the filtrate did not suffer from an induction period, whereas the one catalyzed by the virgin material did. This experiment clearly shows that the palladium becomes detached from the support, presumably via reduction to Pd(0). Thus, it is not the palladacycle itself that catalyzes the reaction and this clearly disproves the notion of a Pd(II)/Pd(IV) cycle. As ligand-free palladium must now be the catalyst, it is obvious that the mechanism is the same as in the ligand-free reactions described above.

Beletskaya in her work on nitrogen-containing palladacycles already commented that these were only the precursors of a Pd(0) species, based on the observation of induction periods and sigmoidal kinetic curves [33].

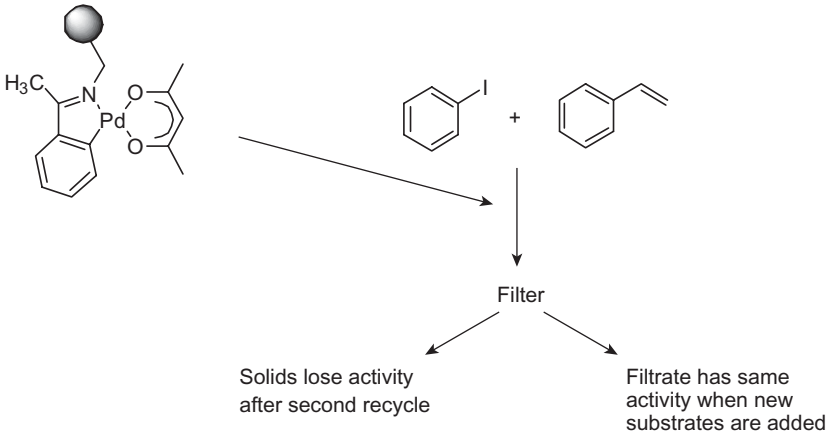

Scheme 3.6 Attempted recycle of an immobilized palladacycle reveals its instability.

De Vries and coworkers compared the rate of the Hermann–Beller palladacycle with their own homeopathic palladium method at the same S/C ratio. In these experiments, the catalysts were added to the hot solution containing all other ingredients. Under these circumstances, there hardly is any induction period in both reactions. This would seem to dispel the notion that palladacycles act as a slow release reservoir for Pd(0). Both reactions proceeded at about the same rate [23].

Attempts to create recyclable palladacycle or pincer type catalysts have been most revealing. Thus, Gladysz in an attempt to recycle an imine-based palladacycle carrying fluorous ponytails also found activity transferred to the nonfluorous phase and was able to prove the presence of Pd-colloids using TEM [34]. Several studies have appeared that show beyond doubt that PCP and SCS pincer complexes also decompose during the Heck reaction and lead to the formation of colloidal palladium [35]. Evidence was based on immobilization studies and on the application of the extensive Hg poisoning protocol developed by Finke, which proved the presence of palladium colloids [6].

Thus, the conclusion seems justified that all palladacycles and pincers decompose during the Heck reaction at high temperatures to form palladium colloids. A review by Jones and coworkers very neatly documents a lot of these cases [25].

Many reports have appeared on the use of heterogeneous palladium catalysts in the Heck reaction [25, 36]. Several different carrier materials have been used such as plain carbon, silica, or porous glass; the palladium has been built into the crystal lattice of zeolites, hydroxyapatite, and many other materials. Practically all reports showed that the catalyst could be reused several times and the authors have interpreted this as proof that the reaction takes place at the surface of the catalyst. Some researchers even bothered to do a hot filtration test to check for activity in the homogeneous phase. Most researchers reported that they did not find any activity; again seeming to confirm that the reaction really takes place at the surface of the catalyst and not in solution.

If one bothers to collect the results of all these paper in tabular form, a striking correlation is found: in all cases were the catalyst/substrate ratio was high the TOF was low, and reversely when the catalyst/substrate ratio was low the TOF was high [37]. This result is not easily explained on the basis of surface reactivity only and on the contrary is strongly reminiscent of the behavior of nanoparticle catalysis. Arai was the first to propose that it is indeed the leached palladium species that is responsible for the reaction in his work on the use of supported palladium catalysts in the Heck reaction of iodobenzene and methyl acrylate [38].

By using a three-phase test with an aryl iodide attached to a solid support, Davies was able to show that the Pd/C becomes active in the Heck reaction on butyl acrylate only after addition of a soluble monomeric aryl iodide or bromide [39]. Interestingly, he also found that the rate increased with increasing amounts of NaOAc. This suggests that the heterogeneous catalyst is solubilized by oxidative addition of the aryl halide and enters the catalytic cycle in the form of a soluble anionic species such as $(ArPd[OAc]Br)^-$ or $(ArPd[OAc]_n)^-$. Biffis reported more or less similar findings in the Heck reaction with Pd/Al_2O_3 (AO–Pd) and Pd deposited on an ion-exchange resin containing sulfonate groups (PS–Pd) [40]. Aryl bromide alone was sufficient to solubilize the palladium when AO–Pd was used, but ArBr and NaOAc where necessary with PS–Pd. A review on the use of heterogeneous catalysts in the Heck reaction in which Biffis and Zecca describe the importance of leaching is highly recommended reading [36].

Köhler performed extensive studies on a range of Pd/C catalysts that differed in Pd dispersion, Pd distribution, and oxidation state [41]. He found that most active systems were obtained with catalysts that had high dispersion, low degree of reduction, and uniform Pd impregnation. In addition, sufficient water content was also found to be important. He also concluded that palladium leaching correlates significantly with the reaction parameters. In a later paper, he found that Pd deposited on the zeolite NaY can even be used for the Heck reaction on aryl chlorides in the presence of tetrabutylammonium bromide [42]. Here again a good correlation was found between palladium in solution and the conversion of aryl bromide (Figure 3.6). During the reaction about one-third of the palladium goes into solution, but after the reaction is finished, less then 1 ppm of palladium is found in solution.

Thus, also in the case of heterogeneous palladium catalysts the palladium is dissolved via oxidative addition with aryl halide in the presence of anions to form $ArPdX_2^-$; after running the course of the Heck reaction, the palladium zero that is formed after the beta-hydride elimination remains solubilized in the form of nanoparticles till the end of the reaction when the rate of oxidative addition becomes slow. At this point, all the palladium reprecipitates as clearly shown in Figure 3.4.

Since it is known that $Pd(PPh_3)_4$ spontaneously forms nanoparticles within 1 day even at room temperature [44], it would seem safe to assume that at temperatures above 120 °C all palladium phosphine complexes also convert into nanoparticles. Thus, this type of catalyst is particularly unsuitable for high-temperature Heck reactions as the large excess of ligand with respect to the number of acces-

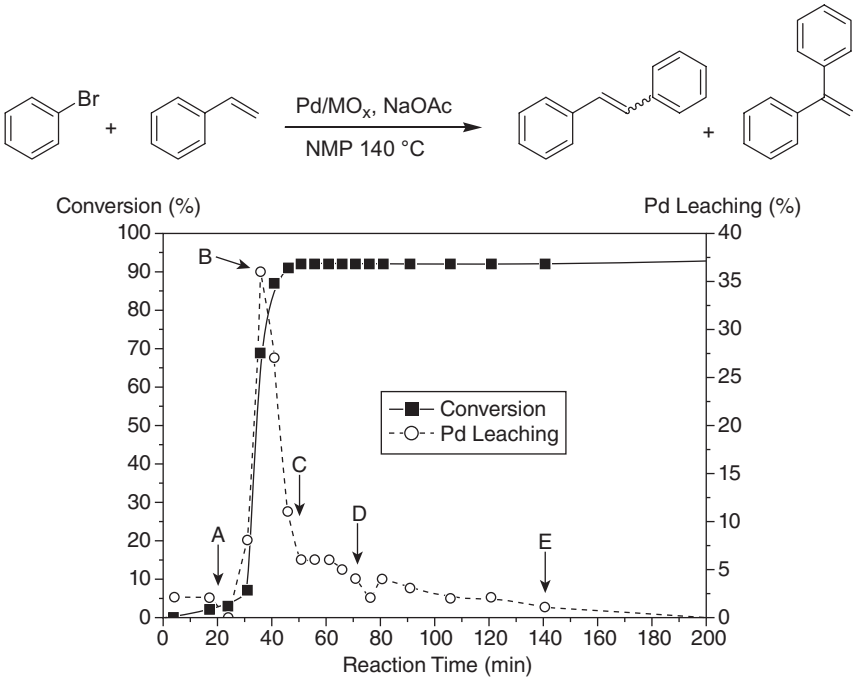

Figure 3.4 Time-dependent correlation of conversion and Pd leaching (percentage of the total Pd amount) in the Heck reaction of bromobenzene and styrene in the presence of Pd/TiO_2 (reaction conditions: 180 mmol bromobenzene, 270 mmol styrene, 216 mmol NaOAc, 0.2 mol% Pd catalyst, 180 mL NMP, 140 °C). Arrows A–E mark typical events during comparable experiments reported up to now (A:, Pd dissolution starting at reaction temperature; B: maximum amount of Pd in solution/highest reaction rate; C: substantial redeposition of Pd onto the support with increasing conversion; D: (far-reaching) completion of Pd redeposition; E: complete redeposition of even Pd traces by increased temperature/reducing agents) (reprinted from Ref. [43]).

sible palladium atoms will lead to a deactivated catalyst. Palladium NHC complexes are also known to form nanoparticles at high temperatures [45]. In conclusion, in view of the above we have to assume that the same mechanism of palladium nanoparticles and anionic intermediates is operative in all Heck–Mizoroki reactions at high temperatures, regardless of the type of palladium precursor.

3.2.2
The Kumada–Corriu Reaction

The Kumada–Corriu reaction is a cross-coupling reaction in which an alkyl or aryl Grignard reagent is coupled to an sp^2 carbon atom, usually in the form of an aryl or vinyl halide [46]. The reaction is catalyzed by palladium, nickel, and iron.

De Vries reported the use of ligand-free palladium in the Kumada reaction [47]. The reaction was not very selective and only a low yield of the coupling

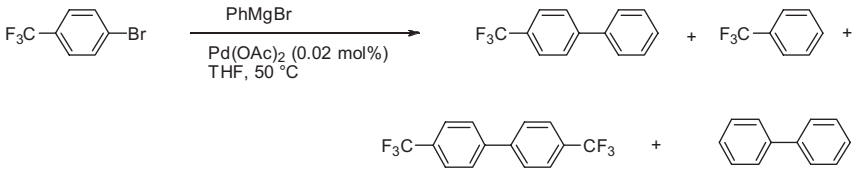

Scheme 3.7 Kumada–Corriu reaction catalyzed by ligand-free palladium.

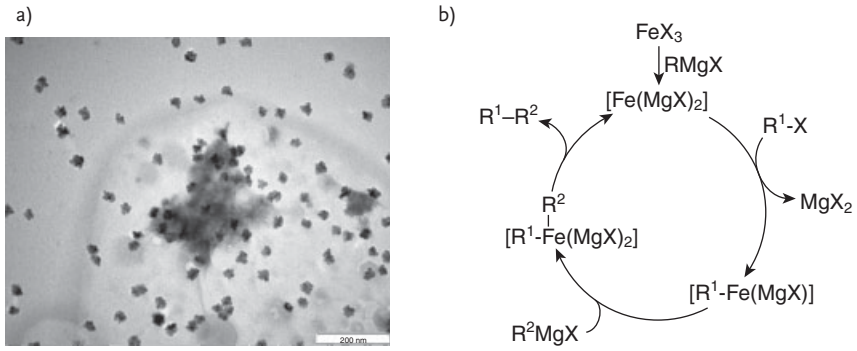

Figure 3.5 (a) TEM of Fe-nanoparticles that were used as catalyst for the Kumada-Corriu reaction by Bedford. (b) Mechanism proposed by Fürstner and coworkers for the iron-catalyzed Kumada–Corriu coupling.

product was obtained. Large amounts of the Grignard homo-coupling product, a small amount of the aryl bromide coupling product, and some reduction product were also obtained (Scheme 3.7). In fact, poor selectivity in the Kumada reaction catalyzed by palladium phosphine complexes may point to instability of the palladium complex used since, normally speaking, use of isolated palladium complexes leads to very high selectivities to the cross-coupling product.

Kochi has reported the use of iron salt as catalyst for cross-coupling reactions, mainly of alkenyl halides [48]. Recently, this chemistry has been taken up again and expanded by Fürstner [49], Cahier [50], Bedford [51], and others [52]. Excellent yields have been obtained in the cross-coupling of Grignards with aryl chlorides, tosylates, and triflates; surprisingly the bromides and iodides are coupled in poor yield, with large amount of the homo-coupling products also formed. Kochi in his first report already mentioned the formation of gray-black solutions upon addition of the Grignard reagent [48]. Bedford, examining the $FeCl_3$-catalyzed coupling between aryl-Grignards and secondary alkyl bromides, examined the dark solution at the end of the reaction using TEM and discovered the presence of iron nanoparticles (Figure 3.5a) [51]. He then showed that preformed iron nanoparticles, stabilized by PEG, are also very efficient catalysts for this reaction. There is still considerable controversy over the mechanism of the iron-catalyzed cross-coupling. Kochi originally proposed a Fe(I)/Fe(III) mechanism, whereas Bedford favored a

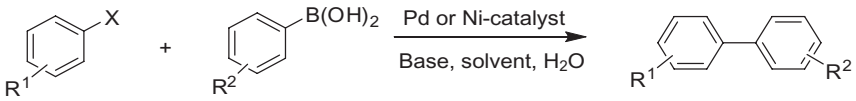

Scheme 3.8 The Suzuki reaction.

single-electron transfer (SET) mechanism based on the outcome of some radical clock-type experiments, which clearly showed that radical intermediates were involved. Fürstner, however, recently proposed a mechanism based on an Fe(–2)/Fe(0) cycle (Figure 3.5b) [53]. DFT calculations performed by Norrby and coworkers support an Fe(I)/Fe(III) mechanism [54].

3.2.3 The Suzuki Reaction

In the Suzuki reaction, the arylating agent is an arylboronic acid or derivative thereof. The reaction is catalyzed by palladium or nickel complexes [55] (Scheme 3.8).

El-Sayed and coworkers showed that the Suzuki reaction on aryl iodides can be catalyzed by palladium nanoparticles stabilized by poly-vinylpyrrolidine (PVP) in water [56]. However, they noted that during the reaction precipitation of palladium black occurred. Nacci and coworkers used palladium nanoparticles in tetraalkylammonium bromides as ionic liquid type solvent [57]. They were able to obtain excellent yields in the Suzuki reaction of aryl bromides and activated aryl chlorides. Many papers have since appeared on the use of different stabilizing agents for palladium nanoparticles used as catalyst in the Suzuki reaction. De Vries and coworkers showed that ligand-free palladium led to excellent results in the Suzuki reaction on aryl bromides with catalysts loadings between 0.01 and 0.05 mol% [47]. The authors presume that also in this case, nanoparticles are present that act as a reservoir of Pd(0). Trzeciak and coworkers used $Pd(OAc)_2$ or $PdCl_2$ immobilized on cyclohexyldiamine-modified glycidyl methacrylate polymer as catalyst in the Suzuki reaction. They examined the catalysts using TEM, SEM, EDX, and XPS. Palladium nanoparticles were formed under the conditions of the Suzuki–Miyaura reaction, the size of which depended on the type of anion. The palladium acetate derived catalyst was found to be fully reduced, leading to the formation of relatively small (2–5 nm) nanoparticles that were highly active. On the other hand, the palladium chloride derived catalyst was only partially reduced, and rather large nanoparticles were formed that had much less activity [58].

Rothenberg and coworkers prepared nanoparticles based on four different metals: Pd, Pt, Cu, and Ru [59]. They tested these nanoparticles and also mixed metal nanoparticles in the Suzuki–Miyaura reaction between iodobenzene and phenylboronic acid in DMF using K_2CO_3 as base (Table 3.1). As expected, palladium displayed the highest activity of the monometallic catalysts, affording quantitative yields after 4 h at 110 °C. No reaction was observed with the platinum

Table 3.1 Biphenyl yields and second-order rate constants obtained using mixed metal nanoparticle catalysts[a].

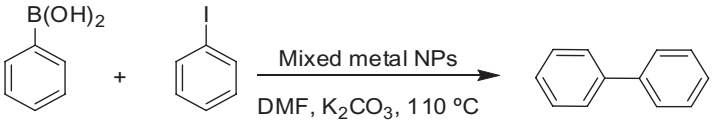

Entry	Catalyst composition	Yield (%)	k_{obs} (L/mol min^{-1})
1	Cu	62	3.2×10^{-3}
2	Pd	100	5.9×10^{-2}
3	Ru	40	2.0×10^{-3}
4	Cu/Pd	100	6.1×10^{-2}
5	Pd/Pt	94	9.7×10^{-3}
6	Pd/Ru	100	2.9×10^{-2}
7	Cu/Pd/Pt	92	2.5×10^{-2}
8	Cu/Pd/Ru	100	3.8×10^{-2}
9	Pd/Pt/Ru	81	7.3×10^{-3}
10	Cu/Pd/Pt/Ru	62	2.8×10^{-3}

a) Standard reaction conditions: 0.50 mmol iodobenzene, 0.75 mmol phenylboronic acid, 1.5 mmol K_2CO_3, 0.01 mmol catalyst (2 mol% total metal nanoclusters relative to PhI), 12.5 mL DMF, N_2 atmosphere, 110 °C.

clusters, but ruthenium and, surprisingly, copper clusters were found to be both active and stable. Of the bimetallic combinations, Cu/Pd was the most active, on par with pure Pd nanoparticles.

Leadbeater and coworkers reported a metal-free Suzuki reaction carried out in a microwave at >160 °C [60]. Later, these results were retracted as the authors found that the reaction was actually catalyzed by ppb amounts of palladium that were present as impurity in Na_2CO_3 that was used as the base [61]. This is of course in line with the earlier findings that the higher the substrate/catalyst ratio, the higher the TOF.

Gladysz used a palladacycle decorated with fluorous ponytails as catalyst in the Suzuki reaction. He found that catalyst activity transferred from the fluorous phase to the DMF phase [34]. This phase showed a characteristic orange-red color that suggested the presence of nanoparticles. In addition, upon repeated recycle the palladacycle catalyst completely lost its activity. TEM showed the presence of palladium nanoparticles. Similarly, Bedford developed a silica immobilized palladacycle, which was used as catalyst in the Suzuki reaction (Figure 3.6). The catalyst lost activity upon each recycle, and the authors were able to show that the palladacycle ligand is arylated leading to the formation of palladium nanoparticles [62].

Nájera compared the rate of the Suzuki reaction catalyzed by the acetophenone-oxime based palladacycle she developed previously with that of $Pd(OAc)_2$. Interestingly, the rates were very similar in the Suzuki reactions of aryl bromides, suggesting a mechanism which is the same for both catalyst precursors and pre-

sumably involves palladium nanoparticles. However, in the Suzuki reaction of unactivated aryl chlorides the palladacycle gave much better results, suggesting a different mechanism [63].

Not much mechanistic research has been performed on Suzuki reactions catalyzed by palladium nanoparticles. An interesting study was recently published by Fairlamb, Lee, and coworkers [64]. They studied the Suzuki reaction catalyzed by preformed palladium nanoparticles, stabilized by PVP. Using a range of nanoparticles of different size, they found that the normalized TOF did change as function of the total number of accessible palladium atoms; however, they did not change as a function of the number of defect sites (Figure 3.7). Next, they investigated the

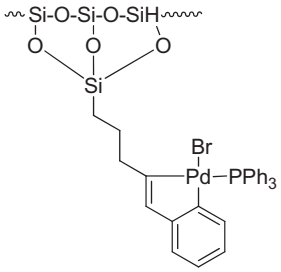

Figure 3.6 Bedford's immobilized palladacycle.

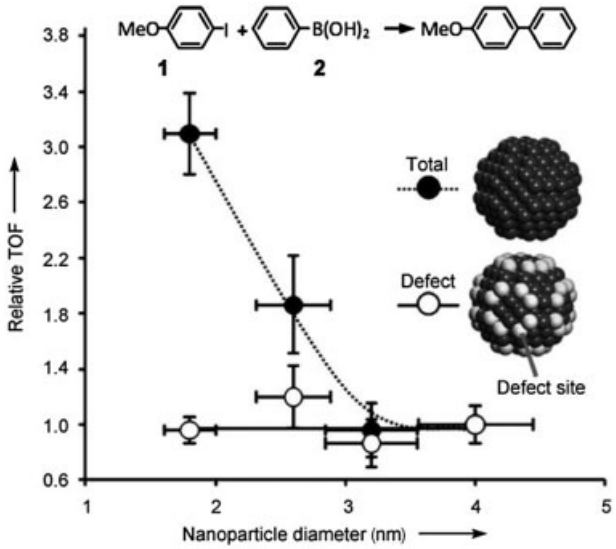

Figure 3.7 Structure-sensitive Suzuki coupling of 1 and 2 over size selected, cubeoctahedral, PVP-stabilized Pd nanoparticles. Turnover frequencies are normalized relative to the surface-atom densities of the largest nanoparticle: total surface atoms (•) or defect surface atoms (◦). The normalized cross-coupling rate should be independent of nanoparticle size if the correct active site has been identified (reprinted from Ref. [64]).

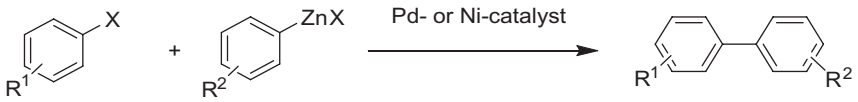

Scheme 3.9 The Negishi coupling.

change in size of the nanoparticles during the Suzuki reaction using EXAFS. They found no change, which led them to conclude that in contrast to the Heck reaction, the catalytic cycle actually takes place at the surface of the nanoparticles on the defect sites.

3.2.4
The Negishi Reaction

In the Negishi coupling, the arylating agent is an arylzinc halide (Scheme 3.9).

There are no reports on the use of preformed palladium nanoparticles as catalyst in the Negishi reaction. De Vries and coworkers showed that ligand-free palladium at 0.02 mol% actually was a good catalyst for Negishi reactions on aryl iodides and activated aryl bromides. Some homo-coupling side products were also formed [47].

Marder and coworkers also described the use of ligand-free palladium acetate as catalyst in the Negishi reaction using stoichiometric tetra-alkylammonium bromide as cocatalyst [65]. The reaction is very fast at room temperature and is completed in seconds; even at –20 °C the reaction was finished in just 30 min. At this temperature, the reaction kinetics shows the characteristic sigmoidal curve. The effect of the palladium concentration on the rate of the reaction was also investigated and again the TOF clearly increased at higher substrate catalyst ratios. They found the reaction was effectively retarded by the addition of only 0.5 eq. of PPh_3, which clearly indicate the involvement of nanoparticles in the catalysis.

3.2.5
The Sonogashira Reaction

In the Sonogashira reaction, a terminal alkyne is coupled to an aryl or alkenyl halide catalyzed by a catalytic system that consists of a homogeneous palladium catalyst, a copper(I) salt, and a secondary amine [66]. As the copper-salt also catalyzes the Glaser-type homo-coupling of the alkyne to form diynes, much work has been done on copper-free Sonogashira reactions, with great success.

Hyeon and coworkers examined the efficacy of both palladium nanoparticles as well as mixed Pd–Ni nanoparticles in the Sonogashira reaction [67]. The mixed nanoparticles were of the core/shell type with the core being mostly nickel and the shell mostly palladium (case c in Figure 3.8). As expected, the core/shell nanoparticles were more active on a palladium basis than the pure palladium nanoparticles as in the latter case most palladium was inside the nanoparticles

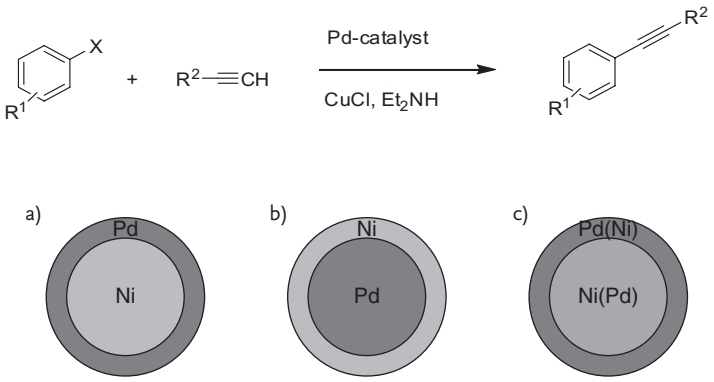

Figure 3.8 Mixed palladium-nickel nanoparticles as catalysts for the Sonogashira reaction.

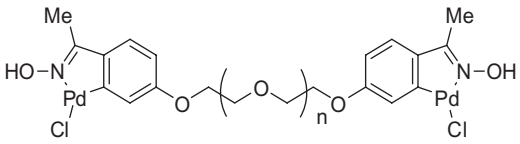

Figure 3.9 Nájera's palladacycle immobilized on PEG by Corma and coworkers.

and unavailable for catalysis. In a similar vain, Srinivasan and coworkers examined the effect of ultrasound on the rate of the Sonogashira reaction of aryl iodides and activated aryl bromides catalyzed by palladium nanoparticles in both acetone and ionic liquids [68]. They found that the reaction proceeded smoothly at 30 °C in high yield under the ultrasound conditions if 2 mol% of $PdCl_2$ was used as precatalyst. In acetone, the reaction was complete within 20 min, whereas in ionic liquids this took 2 h. However, the yields were somewhat higher in the ionic liquids. If no ultrasound was used at this temperature, the reaction did not proceed. However, if $PdCl_2$ was pretreated with ultrasound in the presence of Et_3N after which the reaction was carried out in silent mode, the yields were much lower. This shows that the ultrasound is important both to create an active catalyst, presumably by reducing the size of the Pd–Np's, but it also catalyzes the reaction itself, presumably caused by the local high temperatures and pressures in the cavitations.

A number of groups have reported the use of palladacyles and pincers as catalyst for the Sonogashira reaction. Corma and coworkers attached the palladacycle developed by Nájera and coworkers onto polyethylene glycol (Figure 3.9) [69]. They used this catalyst (5 mol%) in the Sonogashira reaction of *p*-bromoacetophenone and phenylacetylene at 150 °C. Although the catalyst could be reused up to 10 times, they did notice that palladium nanoparticles were formed. They also investigated the change in size of the nanoparticles over the repeated use and found

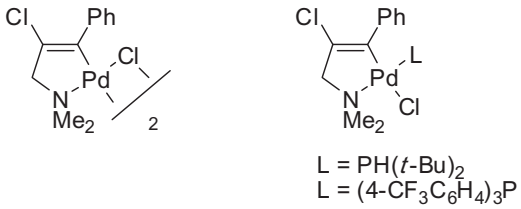

Figure 3.10 Dupont's palladacyles.

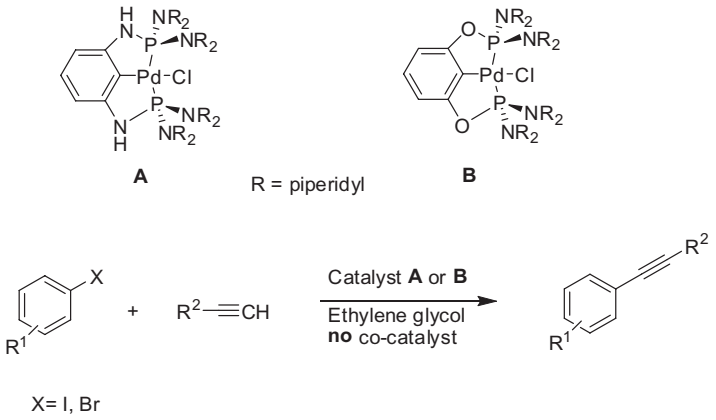

Figure 3.11 Pincers as precatalysts in the Sonogashira reaction.

that the size of the nanoparticles increased only gradually, which they attributed to the stabilizing effect of the polyethylene glycol.

Dupont and coworkers investigated the use of three different palladacyles as catalyst for the Sonogashira reaction between alkynes and aryl iodides as well as activated aryl bromides (Figure 3.10) [70]. At temperatures around 120 °C, these palladacycles were extremely active even at S/C ratios as high as 5×10^5. They performed a series of tests to ascertain the true nature of the catalyst. They found that the catalysis was completely inhibited when 300 eq. of Hg was added. Also, in the Collmann test, which uses an immobilized substrate, they found full activity confirming that the catalyst is a soluble palladium species. Thus the catalyst clearly is a soluble Pd(0) species.

Bolliger and Frech explored the use of palladium PCP–pincer complexes as catalyst in the Sonogashira reaction (Figure 3.11) [71]. The catalysts were highly active at 140 °C in the copper-free Sonogashira coupling of aryl iodides at 50 ppm. Under similar conditions, aryl bromides were coupled using 100 ppm of catalyst. The kinetics of the reactions clearly showed sigmoidal curves. In addition, the TOF of the reactions increased at higher S/C ratios. However, based on a negative mercury test and the fact that the reaction was not accelerated by the addition of PEG or tetra-alkylammonium halides, the authors decided that nanoparticles were not

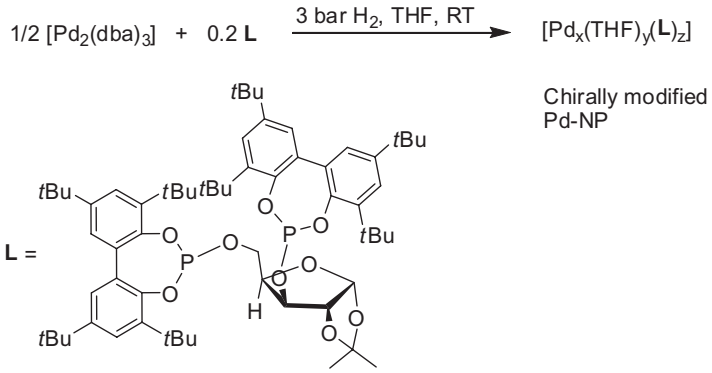

Scheme 3.10 Preparation of chiral palladium nanoparticles.

involved. It should be noted, however, that the mercury test is rather tricky and needs a large excess of mercury as well as very good stirring.

3.2.6
Allylic Alkylation

Asymmetric allylic alkylation is a well-studied reaction that is catalyzed by several classes of transition metal complexes [72]. Much work has been performed with palladium complexes and enantioselectivity can reach up to 99% in selected cases.

Chung and coworkers showed that preformed palladium nanoparticles are in fact excellent catalysts for the allylation of a substituted malonic diester using allyl acetate [73]. Gómez and coworkers reported the asymmetric allylic alkylation of racemic 3-acetoxy-1,3-diphenylpropene with dimethyl malonate using palladium nanoparticles that were modified with a chiral bulky bisphosphite ligand (Scheme 3.10) [74]. They compared the activity and selectivity of this catalyst with the catalyst made from $(Pd[C_3H_5]Cl)_2$ and the same bulky bisphosphite ligand. Although with both systems the product was obtained with 97% ee, there was a striking kinetic difference. The colloidal catalyst on the one hand performed the reaction as a kinetic resolution with a maximum of 56% conversion after 24 h, which had not changed much after 165 h (Table 3.2, Entries 1 and 2). Consequently, the unconverted allylic acetate was obtained with 89% ee. The homogeneous catalyst on the other hand converted the substrate completely without any kinetic resolution in just 1.5 h. Addition of mercury or CS_2 totally inhibited the reaction with the colloidal catalyst, but not the reaction with the palladium complex.

On the other hand, Diéguez and coworkers prepared a series of palladium nanoparticles stabilized by five chiral sugar-based oxazolinyl–phosphite ligands, containing various substituents at the oxazoline and phosphite moieties [75]. These nanoparticles were applied in the Pd-catalyzed asymmetric allylic alkylation and Heck coupling reactions. A detailed study to elucidate the nature of the active species using a continuous-flow membrane reactor (CFMR), accompanied by TEM

Table 3.2 Allylic alkylation catalyzed by chiral nanoparticles.

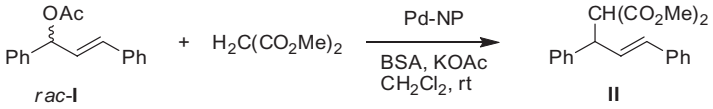

rac-**I** **II**

Entry	I/Pd/L	Time (h)	Conv. (%)	ee (II)	ee (I)
1	100:1:0.2	24	56	97 (*S*)	89 (*S*)
2	100:1:0.2	168	59	97 (*S*)	89 (*S*)
3	100:1:1.05	168	61	97 (*S*)	89 (*S*)

observations, classical poisoning experiments, and kinetic measurements was carried out. The membrane in the reactor had a cut-off of 700 Da allowing only molecular species to pass through. The allylic alkylation reaction with the chiral palladium nanoparticles was performed in the membrane reactor. Analysis of the solution collected during the first two reactor volumes pumped through the reactor showed a conversion of 10% with 19% enantioselectivity. They observed that the catalytic activity stopped after six reactor volumes. To the solution from the first two reactor volumes, 2 mg of KOAc were added and this sample was allowed to stir for a further 4 h. This led to an increase in conversion up to 32% while maintaining the same enantioselectivity. This is in agreement with the fact that the active species are molecular complexes that arise from leaching from the nanoparticles.

Indeed, in view of the mechanism of the reaction, in which an oxidative addition occurs on Pd(0), leaching of a monomeric palladium complex from the nanoclusters as in the Heck reaction seems highly likely.

3.3
Nanoparticles vs. Homogeneous Catalysts in Hydrogenation Reactions

While homogeneous hydrogenation usually is catalyzed by metal complexes in which the metal is oxidized, in heterogeneous catalysis and catalysis with nanoparticles the metal is in the zero oxidation state. If the transition metal complex somehow is reduced to a zero oxidation state complex, the transition to nanoparticles and heterogeneous catalysis is an easy one. Many examples have been documented, but often as a side remark noting that a black precipitate had formed at the end of the reaction.

3.3.1
Hydrogenation of Arenes

While the hydrogenation of benzo-fused heteroaromatic compounds and some heteroaromatic compounds such as furans and pyrroles using homogeneous tran-

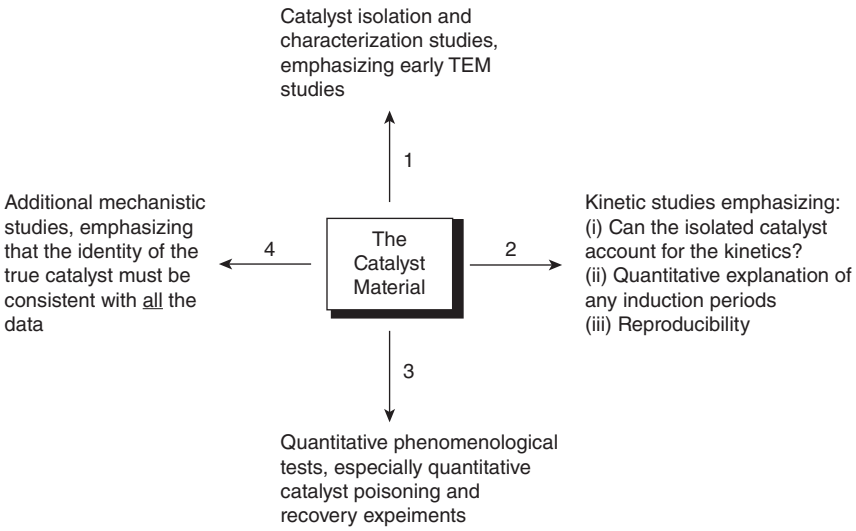

Scheme 3.11 Finke's methodology for distinguishing between homogeneous catalysis and nanocatalysis (or heterogeneous catalysis).

sition metal catalysts is well-documented, the hydrogenation of simple arenes is rare [76]. According to Finke, the only examples of well-established, monometallic, homogeneous catalysts for the hydrogenation of benzene are those developed by Rothwell and coworkers based on Nb(V) and Ta(V) hydrido complexes [77]. Finke has published extensively on hydrogenations catalyzed by homogeneous ruthenium complexes where the true catalysts turned out to be heterogeneous or in the form of soluble nanoparticles. In one case he examined the hydrogenation of benzene using ($Ru[C_6Me_6][OAc]_2$) as precatalyst. Based on the kinetics (sigmoidal curves), poisoning experiments and separately testing a black precipitate versus a red solution for activity, he established that in this case the true catalyst was heterogeneous in nature [77]. The Finke methodology is summarized in Scheme 3.11.

Dyson showed that a homogeneous ruthenium catalyst operating in a two-phase aqueous organic system actually increased in rate upon increasing pH (Scheme 3.12) [78]. He found the increase in rate correlated with the increased formation of ruthenium nanoparticles. Indeed many authors have noted that in aqueous two-phase system, the chances of forming colloids and/or heterogeneous metal are much increased [79].

One reason for the inability of monometallic transition metal catalysts to hydrogenate arenes is the assumption that a three metal ensemble that can be positioned ideally on the three double bonds of the benzene ring is necessary to reduce the first double bond [79]. For this reason, it was generally believed for a long time that triruthenium clusters are indeed truly homogeneous arene hydrogenation catalysts. Süss-Fink and coworkers had reported that ($Ru_3[\mu_2\text{-}H]_3[\eta^6\text{-}C_6H_6][\eta^6\text{-}C_6Me_6]_2[\mu_3\text{-}O])^+$ (Figure 3.12) is an excellent catalyst for the hydrogenation of benzene

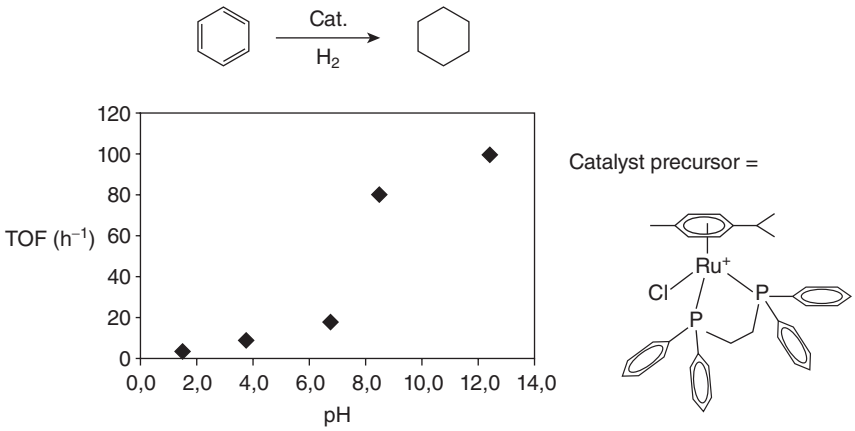

Scheme 3.12 Effect of pH upon rate in the hydrogenation of benzene to cyclohexene (reprinted with permission from Ref [78]).

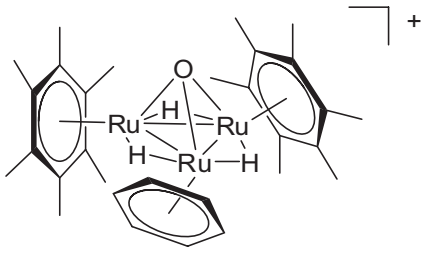

Figure 3.12 Triruthenium cluster.

to cyclohexene at 110 °C, 60 bar H_2, in water with a TOF of 289 h^{-1} and a total turnover (TTO) value of 740 after 2.5 h [80].

Furthermore, the catalyst could be reisolated at the end of the hydrogenation reaction in 95% yield, seemingly confirming its homogeneous nature. However, in a collaboration between the labs of Süss-Fink and Finke, it was shown that the missing 5% of catalyst was found back as a thin metal film on the walls of the reactor. The metal film proved to be a competent catalyst for the hydrogenation of benzene [81]. A series of experiments, including kinetics (sigmoidal curves), poisoning experiments, and the fact that H-D exchange which took place under the catalytic conditions did not involve the triruthenium cluster, showed that in this case it is probably ruthenium nanoparticles or heterogeneous ruthenium that is the real catalyst. Another interesting observation was the extremely fast hydrogenation of ethylbenzene, which was caused by contamination of this substrate with the hydroperoxide PhCH(Me)OOH, which accelerated the decomposition of the ruthenium cluster to form ruthenium nanoparticles.

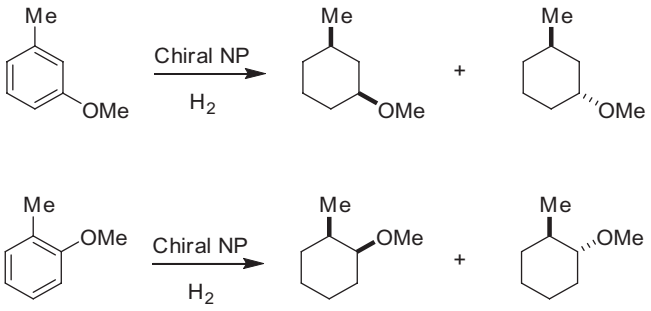

Scheme 3.13 Attempted asymmetric hydrogenation of substituted arenes.

3.3.2
Asymmetric Hydrogenation

Thus far there are no reports on the homogeneous asymmetric hydrogenation of substituted arenes, in line with Finke's suggestion that most homogeneous catalysts are incapable of aromatic hydrogenation. Philippot and coworkers examined the asymmetric hydrogenation of substituted anisoles using ruthenium, rhodium, and iridium nanoparticles stabilized by chiral 1,3-bisphophite ligands based on 1,3-pentanediol or on protected sugar derivatives [82]. The substrates were hydrogenated in good yields with excellent *cis*-selectivity. However, enantioselectivity in these reactions was barely measurable at mostly 6% (Scheme 3.13).

3.4
Platinum-Catalyzed Hydrosilylation

Many reports exist on the hydrosilylation reaction of olefins, catalyzed by homogeneous platinum catalysts [83]. In industry, this reaction is used in the synthesis of silane coupling agents and UV screeners. It is also utilized for the formation of three-dimensional networks via cross-linking between silicone hydride polymers with silicon vinyl polymers. Products are silicone rubbers, liquid injection molding compounds, paper-release coatings, and pressure-sensitive adhesives. Commonly used catalysts are Speier's catalyst (H_2PtCl_6 in isopropanol), $Pt(COD)_2$, and Karstedt's catalyst (Figure 3.13).

Although Chalk and Harrod had proposed a universally accepted mechanism along conventional lines involving discreet homogeneous monometallic complexes via oxidative addition of the silylhydride to the metal catalyst, there were a number of unexplained phenomena [84]. One of these was the catalytic effect of oxygen. The second one was the observation of an induction period, followed by an extremely fast reaction with TOFs in excess of $100\,000\,h^{-1}$. Marciniec and James found that when ruthenium phosphine complexes were used as catalyst, the oxygen served to oxidize the phosphine ligands [85]. Loss of ligands may

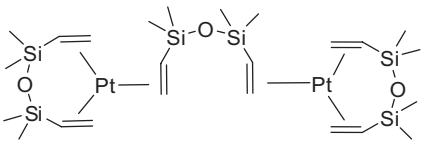

Figure 3.13 Karstedt's catalyst.

well be the start of nanoparticle formation although the authors did not mention this possibility. Lewis examined the reaction catalyzed by $Pt(COD)_2$ and found that upon addition of $(EtO)_3SiH$ a dark solution formed. TEM showed the presence of nanoparticles [86]. The preformed colloidal catalyst was actually faster than the catalyst precursor in the hydrosilylation reaction. Also in the case of Speier's catalyst, he was able to show the presence of nanoparticles. Interestingly, Speier's catalyst is almost an order of magnitude slower than $Pt(COD)_2$ in the hydrosilylation of $TMSCH{=}CH_2$ with $(EtO)_3SiH$. This was readily explained by the difference in size between the nanoparticles. Speier's catalyst was reduced to nanoparticles with an average size of 83 nm, whereas $Pt(COD)_2$ was reduced to much smaller particles, readily explaining the difference in reactivity. Lewis also showed that addition of mercury completely inhibited the catalyst, again confirming the fact that the platinum nanoparticles were indeed the effective catalyst. They noticed that in the absence of oxygen, the catalyst solutions turned darker over time with catalysis slowing down. Thus the oxygen seemed to play a role in keeping the size of the nanoparticles small, possibly as a ligand.

However, in a remarkable turnaround Lewis and coworkers distanced themselves from this mechanism based on the involvement of nanoparticles in spite of all the evidence [87]. This was mainly based on a study of the mechanism of the hydrosilylation reaction catalyzed by Karstedt's catalyst in which they made use of EXAFS, SAXS, and UV-vis. Regardless of the hydrosilane olefin ratio, they found that the catalyst during the reaction is a monomeric platinum compound containing one silicon and carbon in the first coordination sphere. The final platinum compound is a function of the ratio between the olefin and the hydrosilylating agent. At excess olefin, the platinum "end product" contains only platinum carbon bonds, whereas in the presence of excess hydrosilylating agent the platinum end product is multinuclear and contains only platinum silicon bonds. They find that oxygen functions by disrupting multinuclear platinum species that are formed when poorly coordinating olefins are used. The mechanism they proposed is depicted in Scheme 3.14.

3.5 Conclusions

It is clear from the many examples cited above that distinguishing between a mechanism in which a monomeric metal complex is the catalyst and a mechanism

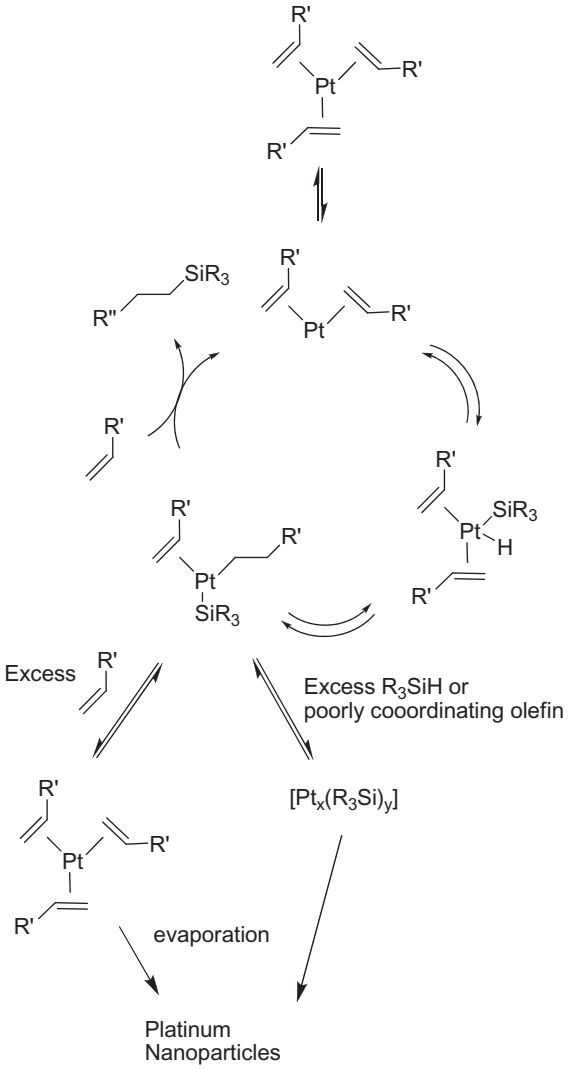

Scheme 3.14 Proposed mechanism for the platinum-catalyzed hydrosilylation.

in which metal nanoparticles are the catalyst is not always easy. The obvious (visible) presence of one form does not rule out the catalytic activity of the other form. Kinetics helps; the observation of sigmoidal curves is often a tell-tale sign of catalysis by nanoparticles or even a heterogeneous catalyst. Another clue is the observation of an increase in TOF with increasing substrate/catalyst ratio. EXAFS is a very powerful technique as it allows the observation of metal species during the catalytic reaction. In particular, it can be used to determine their oxidation state and the number of other atoms the average metal atom is surrounded with.

Thus the metal–metal number, which is an indication of nanoparticle formation, can be easily determined. This can even be followed over time. Poisoning studies can help to validate that the catalysis takes place at a surface rather than via a homogeneous complex. Observation of nanoparticles via TEM by itself should not be considered as conclusive evidence, but their absence is rather a strong evidence for a mechanism via a monometallic complex.

Nanoparticle catalysis has some obvious advantages as well as disadvantages when compared to catalysis with discreet metal complexes. Obvious advantage is the fact that no expensive ligands are used, which in addition simplifies the purification of the product. At the end of the reaction, the nanoparticles usually precipitate, which makes catalyst separation from the product quite easy. Many new developments are expected from this field.

References

1 Horvath, I.T. (ed.) (2003) *Encyclopedia of Catalysis*, vol. 1–6, John Wiley & Sons, Inc., New York.

2 van Leeuwen, P.W.N.M. (2004) *Homogeneous Catalysis. Understanding the Art*, Kluwer Academic Publishing, Dordrecht.

3 Ertl, G., Knözinger, H., Schüth, F., and Weitkamp, J. (eds) (2008) *Handbook of Heterogeneous Catalysis*, vol. 1–8, 2nd edn, Wiley-VCH Verlag GmbH, Weinheim.

4 Astruc, D. (ed.) (2008) *Nanoparticles and Catalysis*, Wiley-VCH Verlag GmbH, Weinheim.

5 Arends, I.W.C.E., and Sheldon, R.A. (2001) *Appl. Catal. A Gen.*, **212**, 175.

6 Widegren, J.A. and Finke, R.G. (2003) *J. Mol. Catal. A Chem.*, **198**, 317–341.

7 (a) Oestreich, M. (ed.) (2009) *The Mizoroki-Heck Reaction*, Wiley-VCH Verlag GmbH, Weinheim; (b) Beletskaya, I.P. and Cheprakov, A.V. (2000) *Chem. Rev.*, **100**, 3009.

8 (a) Heck, R.F. and Nolley, J.P., Jr. (1972) *J. Org. Chem.*, **37**, 2320; (b) Heck, R.F. (1982) *Org. React.*, **27**, 345.

9 Reetz, M.T., Breinbauer, R., and Wanninger, K. (1996) *Tetrahedron Lett.*, **37**, 4499.

10 Beller, M., Fischer, H., Kühlein, K., Reisinger, C.P., and Herrmann, W.A. (1996) *J. Organomet. Chem.*, **520**, 257.

11 Reetz, M.T. and Westermann, E. (2000) *Angew. Chem. Int. Ed.*, **39**, 165.

12 (a) Jeffery, T. (1996) *Advances in Metal-Organic Chemistry*, vol. 5 (ed. L.S. Liebeskind), JAI Press, Greenwich, CT, USA, p. 153; (b) Jeffery, T. (1996) *Tetrahedron*, **52**, 10113.

13 Stephan, M.S., Teunissen, A.J.J.M., Verzijl, G.K.M., and de Vries, J.G. (1998) *Angew. Chem. Int. Ed. Engl.*, **37**, 662.

14 Jutand, A., Negri, S., and de Vries, J.G. (2002) *Eur. J. Inorg. Chem.*, 1711.

15 de Vries, J.G. (2006) *Dalton Trans.*, 421–429.

16 Amatore, C. and Jutand, A. (2000) *Acc. Chem. Res.*, **33**, 314.

17 de Vries, A.H.M., Parlevliet, F.J., Schmieder-van de Vondervoort, L., Mommers J.H.M., Henderickx, H.J.W., Walet, M.A.N., and de Vries, J.G. (2002) *Adv. Synth. Catal.*, **344**, 996.

18 Evans, J., O'Neill, L., Kambhampati, V.L., Rayner, G., Turin, S., Genge, A., Dent, A.J., and Neisius, T. (2002) *J. Chem. Soc. Dalton Trans.*, 2207.

19 Reetz has shown that acetate itself can function as reductant: Reetz, M.T., and Lohmer, G. (1996) *Chem. Commun.*, 1921. In the case of benzoic anhydride the authors detected the formation of chloroacrylate esters, which points in the direction of a Wacker type mechanism for the reduction [13]. This latter mechanism has also been proposed by Heck [8b].

20 Carrow, B.P. and Hartwig, J.F. (2010) *J. Am. Chem. Soc.*, **132**, 79.

21 Schmidt, A.F., Al-Halaiqa, A., Smirnov, V.V., and Kurokhtina, A.A. (2008) *Kinet. Catal.*, **49**, 638.

22 Schmidt, A.F. and Smirnov, V.V. (2003) *J. Mol. Catal. A Chem.*, **203**, 75.

23 de Vries, A.H.M., Mulders, J.M.C.A., Mommers, J.H.M., Henderickx, H.J.W., and de Vries, J.G. (2003) *Org. Lett.*, **5**, 3285.

24 Arvela, R.K. and Leadbeater, N.E. (2005) *J. Org. Chem.*, **70**, 1786.

25 Phan, N.T.S., Van Der Sluys, M., and Jones, C.W. (2006) *Adv. Synth. Catal.*, **348**, 609.

26 Kleist, W., Pröckl, S.S., and Köhler, K. (2008) *Catal. Lett.*, **125**, 197.

27 Beller, M., Fischer, H., Herrmann, W.A., Öfele, K., and Broßmer, C. (1995) *Angew. Chem. Int. Ed. Engl.*, **34**, 1848; (b) Herrmann, W.A., Broßmer, C., Reisinger, C.-P., Riermeier, T.H., Öfele, K., and Beller, M. (1997) *J. Am. Chem. Soc.*, **119**, 1357.

28 (a) Dupont, J., Pfeffer, M., and Spencer, J. (2001) *Eur. J. Inorg. Chem.*, 1917; (b) Beletskaya, I.P. and Cheprakov, A.V. (2004) *J. Organomet. Chem.*, **689**, 4055; (c) Dupont, J., Consorti, C.S., and Spencer, J. (2005) *Chem. Rev.*, **105**, 2527; (d) Bedford, R.B., Cazin, C.S.J., and Holder, D. (2004) *Coord. Chem. Rev.*, **248**, 2283.

29 Shaw, B.L. (1998) *New J. Chem.*, 77.

30 Louie, J. and Hartwig, J.F. (1996) *Angew. Chem. Int. Ed. Engl.*, **35**, 2359.

31 (a) Beller, M. and Riermeier, T.H. (1998) *Eur. J. Inorg. Chem.*, 29; (b) Böhm, V.P.W. and Herrmann, W.A. (2001) *Chem. Eur. J.*, **7**, 4191; (c) Rosner, T., Bars, J.L., Pfaltz, A., and Blackmond, D.G. (2001) *J. Am. Chem. Soc.*, **123**, 1848.

32 Nowotny, M., Hanefeld, U., van Koningsveld, H., and Maschmeyer, T. (2000) *Chem. Commun.*, 1877.

33 Beletskaya, I.P., Kashin, A.N., Karlstedt, N.B., Mitin, A.V., Cheprakov, A.V., and Kazankov, G.M. (2001) *J. Organomet. Chem.*, **622**, 89.

34 (a) Rocaboy, C. and Gladysz, J.A. (2002) *Org. Lett.*, **4**, 1993; (b) Rocaboy, C. and Gladysz, J.A. (2003) *New J. Chem.*, **27**, 39.

35 (a) Yu, K., Sommer, W., Richardson, J.M., Weck, M., and Jones, C.W. (2004) *Adv. Synth. Catal.*, **347**, 161; (b) Eberhard, M.R. (2004) *Org. Lett.*, **6**, 2125; (c) Bergbreiter, D.E., Osburn, P.L. and Frels, J.D. (2005) *Adv. Synth. Catal.*, **347**, 172.

36 Biffis, A., Zecca, M., and Basato, M. (2001) *J. Mol. Catal. A Chem.*, **173**, 249.

37 Dams, M. (2004) Dissertation. Catholic University of Leuven, Belgium.

38 Zhao, F., Bhanage, B.M., Shirai, M., and Arai, M. (2000) *Chem. Eur. J.*, **6**, 843.

39 Davies, I.W., Matty, L., Hughes, D.L., and Reider, P.J. (2001) *J. Am. Chem. Soc.*, **123**, 10139.

40 Biffis, A., Zecca, M., and Barsato, M. (2001) *Eur. J. Inorg. Chem.*, 1131.

41 Pröckl, S.S., Kleist, W., Gruber, M.A., and Köhler, K. (2004) *Angew. Chem. Int. Ed.*, **43**, 1881.

42 Köhler, K., Heidenreich, R.G., Krauter, J.G.E., and Pietsch, J. (2002) *Chem. Eur. J.*, **8**, 622.

43 Djakovitch, L., Köhler, K., and de Vries, J.G. (2008) *Nanoparticles and Catalysis* (ed. D. Astruc), Wiley-VCH Verlag GmbH, Weinheim, p. 303.

44 Ye, E., Tan, H., Li, S., and Fan, W.Y. (2006) *Angew. Chem. Int. Ed.*, **45**, 1120.

45 Inés, B., SanMartin, R., Moure, M.J., and Domínguez, E. (2009) *Adv. Synth. Catal.*, **351**, 2124; (b) Karimi, B.B. and Enders, D. (2006) *Org. Lett.*, **8**, 1237.

46 (a) Tamao, K., Sumitani, K., and Kumada, M. (1972) *J. Am. Chem. Soc.*, **94**, 4374; (b) Corriu, R.J.P. and Massé, J.P. (1972) *J. Chem. Soc. Chem. Commun.*, 144; (c) Ackermann, L. (2009) *Modern Arylation Methods*, Wiley-VCH Verlag GmbH, Weinheim.

47 Alimardanov, A., Schmieder-van de Vondervoort, L., de Vries, A.H.M., and de Vries, J.G. (2004) *Adv. Synth. Catal.*, **346**, 1812.

48 (a) Tamura, M. and Kochi, J.K. (1971) *J. Am. Chem. Soc.*, **93**, 1487; (b) Neumann, S.M. and Kochi, J.K. (1975) *J. Org. Chem.*, **40**, 599.

49 Sherry, B.D. and Fürstner, A. (2008) *Acc. Chem. Res.*, **41**, 1500.

50 (a) Cahiez, G., Chavant, P.Y., and Metais, E. (1992) *Tetrahedron Lett.*, **33**, 5245; (b) Cahiez, G. and Marquais, S. (1996) *Tetrahedron Lett.*, **37**, 1773; (c) Cahiez, G. and Avedissian, H. (1998) *Synthesis*,

1199; (d) Duplais, C., Bures, F., Korn, T., Sapountzis, I., Cahiez, G., and Knochel, P. (2004) *Angew. Chem. Int. Ed.*, **43**, 2968.
51 Bedford, R.B., Betham, M., Bruce, D.W., Davis, S.A., Frost, R.M., and Hird, M. (2006) *Chem. Commun.*, 1398.
52 (a) Bolm, C., Legros, J., Le Paih, J., and Zani, L. *Chem. Rev.*, 2004, **104**, 6217; (b) Shinokubo, H. and Oshima, K. (2004) *Eur. J. Org. Chem.*, 2071; (c) Fürstner, A. and Martin, R. (2005) *Chem. Lett.*, **34**, 624; (d) Correa, A., Mancheno, O.G., and Bolm, C. (2008) *Chem. Soc. Rev.*, **37**, 1108; (e) Czaplik, W.M., Mayer, M., Cvengros, J., and Jacobi von Wangelin, A. (2009) *ChemSusChem*, **2**, 396.
53 Fürstner, A., Martin, R., Krause, H., Seidel, G., Goddard, R., and Lehmann, C.W. (2008) *J. Am. Chem. Soc.*, **130**, 8773.
54 Kleimark, J., Hedström, A., Larsson, P.-F., Johansson, C., and Norrby, P.-O. (2009) *ChemCatChem*, **1**, 152.
55 Miyaura, N. and Suzuki, A. (1995) *Chem. Rev.*, **95**, 2457.
56 Li, Y., Hong, X.M., Collard, D.M., and El-Sayed, M.A. (2000) *Org. Lett.*, **2**, 2385.
57 (a) Calo, V., Nacci, A., Monopoli, A., and Montingelli, F. (2005) *J. Org. Chem.*, **70**, 6040; (b) Calo, V., Nacci, A., and Monopoli, A. (2006) *Eur. J. Org. Chem.*, 3791.
58 Borkowski, T., Trzeciak, A.M., Bukowski, W., Bukowska, A., Tylus, W., and Kępiński, L. (2010) *Appl. Catal. A Gen.*, **378**, 83.
59 Thathagar, M.B., Beckers, J., and Rothenberg, G. (2002) *J. Am. Chem. Soc.*, **124**, 11858.
60 (a) Leadbeater, N.E. and Marco, M. (2003) *Angew. Chem. Int. Ed.*, **42**, 1407; (b) Leadbeater, N.E. and Marco, M. (2003) *J. Org. Chem.*, **68**, 5660.
61 Arvela, R.K., Leadbeater, N.E., Sangi, M.S., Williams, V.A., Granados, P., and Singer, R.D. (2005) *J. Org. Chem.*, **70**, 161.
62 Bedford, R.B., Cazin, C.S.J., Hursthouse, M.B., Light, M.E., Pike, K.J., and Wimperis, S. (2001) *J. Organomet. Chem.*, **633**, 173.
63 (a) Alacid, E., Alonso, D.A., Botella, L., Nájera, C., and Pacheco, M.C. (2006) *Chem. Rec.*, **6**, 117; (b) Alonsa, D.A. and Nájera, C. (2010) *Chem. Soc. Rev.*, **39**, 2891.
64 Ellis, P.J., Fairlamb, I.J.S., Hackett, S.F.J., Wilson, K., and Lee, A.F. (2010) *Angew. Chem. Int. Ed.*, **49**, 1820.
65 Liu, J., Deng, Y., Wang, H., Zhang, H., Yu, G., Wu, B., Zhang, H., Li, Q., Marder, T.B., Yang, Z., and Lei, A. (2008) *Org. Lett.*, **10**, 2661.
66 (a) Sonogashira, K. (2004) *Metal-Catalyzed Cross-Coupling Reactions*, vol. 1 (eds F. Diederich and A. de Meijere), Wiley-VCH Verlag GmbH, Weinheim, p. 319; (b) Chinchilla, R. and Nájera, C. (2007) *Chem. Rev.*, **107**, 874.
67 Son, S.U., Jang, Y., Park, J., Na, H.B., Park, H.M., YunJ, H.J., Lee, J., and Hyeon, T. (2004) *J. Am. Chem. Soc.*, **126**, 5026.
68 Gholap, A.R., Venkatesan, K., Pasricha, R., Daniel, T., Lahoti, R.J., and Srinivasan, K.V. (2005) *J. Org. Chem.*, **70**, 4869.
69 Corma, A., García, H., and Leyva, A. (2006) *J. Mol. Catal.*, **240**, 87.
70 Consorti, C.S., Flores, F.R., Rominger, F., and Dupont, J. (2006) *Adv. Synth. Catal.*, **348**, 133.
71 Bolliger, J.L. and Frech, C.M. (2009) *Adv. Synth. Catal.*, **351**, 891.
72 Trost, B.M. and Crawley, M.L. (2003) *Chem. Rev.*, **103**, 2921.
73 Park, K.H., Son, S.U., and Chung, Y.K. (2002) *Org. Lett.*, **4**, 4361.
74 (a) Jansat, S., Gómez, M., Philippot, K., Muller, G., Guiu, E., Claver, C., Castillón, S., and Chaudret, B. (2004) *J. Am. Chem. Soc.*, **126**, 1592; (b) Favier, I., Gómez, M., Muller, G., Axet, M.R., Castillón, S., Claver, C., Jansat, S., Chaudret, B., and Philippot, K. (2007) *Adv. Synth. Catal.*, **349**, 2459.
75 Diéguez, M., Pàmies, O., Mata, Y., Teuma, E., Gómez, M., Ribaudo, F., and van Leeuwen, P.W.N.M. (2008) *Adv. Synth. Catal.*, **350**, 2583.
76 Bianchini, C., Meli, A., and Vizza, F. (2007) *Handbook of Homogeneous Hydrogenation*, vol. 1 (eds J.G. de Vries and C.J. Elsevier), Wiley-VCH Verlag GmbH, Weinheim, p. 455.
77 Widegren, J.A., Bennett, M.A., and Finke, R.G. (2003) *J. Am. Chem. Soc.*, **125**, 10301.
78 Daguenet, C. and Dyson, P.J. (2003) *Catal. Commun.*, **4**, 153.

79 Dyson, P.J. (2003) *Dalton Trans.*, 2964.

80 Süss-Fink, G., Therrien, B., Vieille-Petit, L., Tschan, M., Romakh, V.B., Ward, T., Dadras, M., and Laurenczy, G. (2004) *J. Organomet. Chem.*, **689**, 1362.

81 Hagen, C.M., Vieille-Petit, L., Laurenczy, G., Süss-Fink, G., and Finke, R.G. (2005) *Organometallics*, **24**, 1819.

82 Gual, A., Godard, C., Philippot, K., Chaudret, B., Denicourt-Nowicki, A., Roucoux, A., Castillón, S., and Claver, C. (2009) *ChemSusChem*, **2**, 769.

83 Marciniec, B. (2005) *Coord. Chem. Rev.*, **249**, 2374.

84 Chalk, A.J. and Harrod, J.F. (1945) *J. Am. Chem. Soc.*, **87**, 16.

85 Gulinski, J., James, B.R., and Marciniec, B. (1995) *J. Organomet. Chem.*, **499**, 173.

86 (a) Lewis, L.N. and Lewis, N. (1986) *J. Am. Chem. Soc.*, **108**, 7228; (b) Lewis, L.N. (1990) *J. Am. Chem. Soc.*, **112**, 5998.

87 Stein, J., Lewis, L.N., Gao, Y., and Scott, R.A. (1999) *J. Am. Chem. Soc.*, **121**, 3693.